Spin-1 two-impurity Kondo problem on a lattice

A. Allerdt, R. Žitko, and A. E. Feiguin

Phys. Rev. B **97**, 045103 — Published 5 January 2018

DOI: 10.1103/PhysRevB.97.045103

Spin-1 two-impurity Kondo problem on a lattice

A. Allerdt,[1] R. Žitko,[2] and A. E. Feiguin[1]

[1]*Department of Physics, Northeastern University, Boston, Massachusetts 02115, USA*
[2]*Jožef Stefan Institute, Jamova 39, SI-1000 Ljubljana, Slovenia*
Faculty of Mathematics and Physics, University of Ljubljana, Jadranska 19, SI-1000 Ljubljana, Slovenia

We present an extensive study of the two-impurity Kondo problem for spin-1 adatoms on square lattice using an exact canonical transformation to map the problem onto an effective one-dimensional system that can be numerically solved using the density matrix renormalization group method. We provide a simple intuitive picture and identify the different regimes, depending on the distance between the two impurities, Kondo coupling J_K, longitudinal anisotropy D, and transverse anisotropy E. In the isotropic case, two impurities on opposite(same) sublattices have a singlet(triplet) ground state. However, the energy difference between the triplet ground state and the singlet excited state is very small and we expect an effectively four-fold degenerate ground state, *i.e.*, two decoupled impurities. For large enough J_K the impurities are practically uncorrelated forming two independent underscreened states with the conduction electrons, a clear non-perturbative effect. When the impurities are entangled in an RKKY-like state, Kondo correlations persists and the two effects coexist: the impurities are underscreened, and the dangling spin-$1/2$ degrees of freedom are responsible for the inter-impurity entanglement. We analyze the effects of magnetic anisotropy in the development of quasi-classical correlations.

I. INTRODUCTION

Magnetic adatoms can be used to tailor the properties of substrates[1–3] and to build nanostructures that could pave the way to magnetic devices with novel functionality including qubits and magnetic memories[4–10]. Exciting pioneering examples include quantum corrals formed by Fe atoms on Cu(111)[11], quantum wires on Au(111) surfaces[12], and more recently, magnetic nanostructures[13], one dimensional atomic chains[14,15], and atomic dimers[16]. Depending on their strength and directionality[17–20], quantum-mechanical effects could lead to the self-assembly of one-dimensional Co chains and Fe superlattices[21,22]. These magnetic nanostructures can also serve as a platform to simulate magnetic quantum matter in the same spirit as cold atomic systems[23–26].

This research field is rapidly developing, but creating new technologies based on magnetic nanostructures requires a deeper knowledge of the interplay between the different degrees of freedom and energy scales in the problem. These vary widely depending on the atomic species and the substrates. Some systems have particularly distinguished properties. For instance, scanning tunneling microscopy (STM) studies found large magnetic anisotropies for single manganese and iron atoms on copper nitride.[27] In addition, the anisotropy can be controlled through a coupling of the spin with a conductive electrode[28]. More recently, a holmium atom on a platinum (111) surface was found to have a very large total angular momentum of $J = 8$.[7].

Most of the theoretical understanding relies on the theory of the single-impurity problem[29] and indirect exchange (Ruderman-Kittel-Kasuya-Yosida – RKKY)[30–33]. The latter, in particular, is based on second-order perturbation theory and leaves aside many important puzzles that arise when correlations are taken into account non-perturbatively. For instance, a remarkable result in early numerical renormalization group (NRG) studies of the two-impurity problem[34–36] with spins $1/2$ indicated the existence of a non-Fermi-liquid (NFL) fixed point. A different NFL fixed point was found in the three-impurity problem in the presence of magnetic frustration[37].

The two-impurity problem has been theoretically studied using a range of techniques, both analytical and numerical. Introduced in 1981, it was first analyzed using perturbative scaling ideas[38]. Our understanding continued to evolve through the application of new methods[39–51] and the development of state of the art experimental setups[16,52–54]. In most studies, the impurities are described either by spin-$\frac{1}{2}$ Kondo model or single-orbital Anderson model[29]. However, typical experiments with adatoms on substrates involve transition-metal atoms with high spin such as iron, cobalt, or manganese.

The minimal model to tackle this problem is the two-impurity Kondo Hamiltonian:

$$H = H_{\rm band} + J_K \left(\vec{S}_1 \cdot \vec{s}_{\rm r_1} + \vec{S}_2 \cdot \vec{s}_{\rm r_2} \right). \qquad (1)$$

where $H_{\rm band}$ is the lattice Hamiltonian for non-interacting electrons, $\vec{S}_i$ are the quantum-mechanical impurity spin operators, and $\vec{s}_{r_i}$ represents the conduction electron's spin at the impurity's coordinate r_i, for impurities $i = 1, 2$.

In this work we focus on spin-1 impurities. A point-like spin-1 impurity coupled to a single conduction electron channel will be "underscreened", *i.e.*, the ground state will have a spin-$1/2$ residual moment[55,56]. In other words, a single electron channel can screen at most one-half unit of spin. This problem has been extensively studied and was exactly solved with the Bethe ansatz for the case of a linear dispersion[57–60], and numerically using the numerical renormalization group (NRG)[61–65] for generic situation. The underscreened nature of the ground state with two-fold degeneracy leads to singular thermodynamic behavior characterized by a singular-Fermi-liquid fixed point[63,66,67]. However, most physical examples have a natural magnetic anisotropy that arises from the local spin-orbit coupling that can be quite large[68–70]. Anisotropy is often modeled by adding a term:

$$H_A = DS_z^2 + E(S_x^2 - S_y^2). \qquad (2)$$

Such interactions emerge as an effective spin Hamiltonian of an orbitally degenerate level from the combination of

spin-orbit coupling and crystal-field splitting according to the point-group symmetry. For $S = 1$, the physics strongly depends on the longitudinal anisotropy D, since it splits the three-fold degeneracy of the free moment into a non-degenerate state ($S_z = 0$) and a pair of states($S_z = \pm 1$). The transverse anisotropy term E is smaller than D, and zero if the point group has a C_N axis with $n \geq 3$. When non-zero, it splits the $S_z = \pm 1$ pair. The transverse anisotropy is particularly important in the context of spin-state life-times and decoherence[71]. The magnetic anisotropy hence determines the effective impurity degrees of freedom and the possible physical mechanisms for their quenching at low temperatures. For example, STM experiments with cobalt atoms ($S = 3/2$) on Cu_2N find Kondo effect even in the presence of a hard axis (positive D) anisotropy[72]. The Kondo effect is observed if the ground state levels are degenerate and connected by $\Delta m = 1$. This occurs only for half-integer spin $S \geq 3/2$ when the anisotropy D is positive. The Kondo effect is absent for iron ($S = 2$) and manganese ($S = 5/2$) that both have negative anisotropy[17,27].

The effects of anisotropy in the single-impurity problem are discussed in detail in Ref. 65 using the NRG and a flat density of states. Although this problem exhibits universal physics that is essentially independent of the band structure[60,73–77], the lattice plays an important role in mediating the inter-impurity coupling and leads to the competition between different effects[79–82]. The complexity in the two-impurity case arises from competing energy scales between the single-impurity screening and the RKKY physics. In addition, for high spin the magnetic anisotropy also plays an important role selecting the relevant degrees of freedom that participate in these screening processes. In order to study this problem on a specific lattice, we use a recently developed computational technique[80] that allows us to exactly solve this problem on large lattices with the aid of the density matrix renormalization group method (DMRG)[83–85]. Our results are exact and provide a deeper understanding of the physics beyond perturbative ideas, accounting for all the many-body effects.

One should mention that the NRG has been applied to the two-impurity Kondo problem in the past. Some early works can be found in Refs. 86–88, as well as more recently in Refs. 81,89. These methods are based on the transformation to the even/odd basis of the hybridization matrix, making it diagonal, and a discretization of the two frequency dependent couplings. The lattice details can, in principle, be fully described through the frequency dependence of these functions which, unfortunately, is highly non-trivial except in the very short-distance and long-distance limits. In fact, they are strongly oscillatory for intermediate distances of prime interest. Most works hence performed additional approximations, thus the detailed information about the lattice was actually lost. One can proceed without any approximation, provided that additional measures are taken to reduce the discretization artifacts (*e.g.* if z-averaging over a large number of interleaved discretization meshes is performed). In practice, the calculations are thus limited to distances of order 3-4 sites, while it is very difficult to accurately capture the asymptotic decay of the RKKY superexchange on somewhat longer length scales.

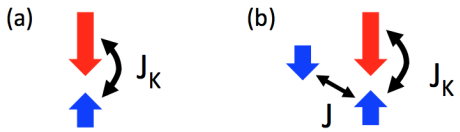

FIG. 1: Toy model representing the strong-coupling limit. Large red arrows represent $S = 1$ impurity spins, while small blue arrows correspond to conduction-band electron spins. (a) A single conduction spin can only partially screen the impurity. (b) A second conduction spin interacts with the first through an antiferromagnetic exchange J. The impurity spin and the second spin favor ferromagnetic alignment.

Therefore, the advantage of our approach consists in being able to robustly describe the range of order 10-20 sites. The limitation is indeed that the lowest energy scale included in the problem is constrained by the finite size error of order $1/L$. This is ultimately the reason for choosing relatively high values of the Kondo exchange coupling J_K: they are chosen such that the spatial extent of the Kondo cloud does not exceed L (and correspondingly that the Kondo temperature T_K is larger than the finite-size error).

The paper is organized as follows: In Section II we present a qualitative overview of the problem from the perspective of the strong-coupling limit. This provides valuable intuition that will help us interpret the numerical results. Section III describes the exact mapping of the model onto an effective one-dimensional problem amenable to DMRG calculations. In Section IV we present our results for both the isotropic and the anisotropic cases. We finally close with a summary and conclusions.

II. QUALITATIVE PICTURE

A. Single spin-1 impurity

1. *Underscreening*

We first propose an intuitive picture to understand the essential physics of the underscreened Kondo problem, focusing on the $S = 1$ single-impurity case, and use a very simple effective model for illustrative purposes. It has been demonstrated in Ref. 90 that in the Kondo problem, only one conduction electron is responsible for the screening. This picture is quite universal. In the weak-coupling limit, one can imagine that this electron is located at the Fermi level[79], while in the strong-coupling limit, it corresponds to the localized orbital directly in contact with the impurity spin. In either case, the remaining conduction electrons form a completely disentangled Fermi sea, and do not play a role in the physics. Therefore, this can be reduced to a problem of an impurity spin (partially) screened by a single conduction electron. In these terms, the $T = 0$ picture for a spin-$1/2$ impurity is of a singlet ground state between both spins while for a spin-1 impurity,

one needs to also account for the extra degrees of freedom and magnetic anisotropy. We refrain from generalizing these ideas to finite temperature, where the many-body screening mechanisms are more complex. We consider the impurity and conduction spins interacting via a Heisenberg exchange J_K, and include the anisotropy as in Eq.(2), see Fig. 1(a). Defining states $|\uparrow\rangle, |\downarrow\rangle$ for the conduction spin, and $|+\rangle, |0\rangle, |-\rangle$ for the impurity spin, one can readily obtain the ground state as a function of D (for now $E = 0$). The Hamiltonian can be diagonalized in blocks, and we focus on the subspaces with total $S^z = m_s = \pm 1/2$. The 2×2 Hamiltonian matrix is:

$$H(m_s = \pm 1/2) = \begin{pmatrix} 0 & \frac{J_K}{\sqrt{2}} \\ \frac{J_K}{\sqrt{2}} & -\frac{J_K}{2} + D \end{pmatrix} \quad . \tag{3}$$

For $D = 0$ we find two degenerate ground states:

$$\begin{aligned} |m_s = 1/2\rangle &\equiv a\,|0\uparrow\rangle - b\,|+\downarrow\rangle\,; \\ |m_s = -1/2\rangle &\equiv a\,|0\downarrow\rangle - b\,|-\uparrow\rangle\,, \end{aligned} \tag{4}$$

with $a = \sqrt{1/3}$ and $b = \sqrt{2/3}$. This degeneracy is a manifestation of underscreening: if one assumes that the spin-1 is actually comprised of two spins $1/2$ (see Fig. 2), the conduction electron will screen only one of them. This leaves a "dangling" spin-$1/2$ that can point in either direction. To make this analogy more explicit, the $S = 1$ states are written in terms of two $S = 1/2$ spins projected onto the $S = 1$ manifold:

$$\begin{aligned} |+\rangle &\equiv |\uparrow\uparrow\rangle \\ |-\rangle &\equiv |\downarrow\downarrow\rangle \\ |0\rangle &\equiv \frac{1}{\sqrt{2}}\left(|\uparrow\downarrow\rangle + |\downarrow\uparrow\rangle\right) \end{aligned} \tag{5}$$

We can readily re-write the eigenstate $|m_s = 1/2\rangle$ as:

$$\begin{aligned} |m_s = 1/2\rangle \;=\; & \frac{1}{\sqrt{6}}\left(|\uparrow\downarrow\rangle|\uparrow\rangle - |\uparrow\uparrow\rangle|\downarrow\rangle\right) + \\ & + \frac{1}{\sqrt{6}}\left(|\downarrow\uparrow\rangle|\uparrow\rangle - |\uparrow\uparrow\rangle|\downarrow\rangle\right). \end{aligned} \tag{6}$$

The two terms in the above sum correspond to two singlets: one between the conduction spin and the first spin, and the other between the conduction spin and the second spin. This can be interpreted as a resonating valence bond (RVB) state with an extra spin always pointing up (see $|\text{Underscreened}\rangle$ in Fig. 3 for a graphical representation of this state). It is easy to show that the entanglement entropy for the impurity is $S = -\frac{1}{3}\log\left(\frac{1}{3}\right) - \frac{2}{3}\log\frac{2}{3}$. These doublet states have also been discussed in the context of quantum dots[91–93].

A similar analysis applies to the $|m_s = -1/2\rangle$ state. The degeneracy of the $|m_s = \pm 1/2\rangle$ states leads to the so-called singular Fermi liquid behavior that emerges when trying to restore the time-reversal symmetry[66]. This can be broken "by hand" by choosing a particular value of S^z. However, the symmetrization of the ground state implies that the self-energy of the problem has to be obtained from two distinct self-energies[67], yielding peculiar low-temperature effects. As soon as an infinitesimal magnetic field is applied, the system picks a unique ground state, and Fermi liquid behavior is restored.

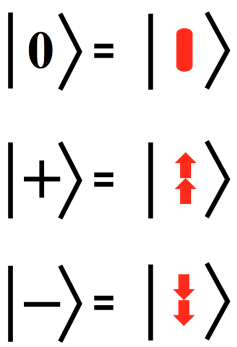

FIG. 2: Graphical representation of three basis states for a single spin $S = 1$ in terms of two spins $S = 1/2$. The $|0\rangle$ state is a triplet with total $S^z = 0$, while the two other states are fully polarized.

The effect of the longitudinal anisotropy D is to change the character of the ground states to more "classical" or "Ising-like" states. $D \gg J_K$ implies $a \gg b$, and the impurity spin has zero total moment. On the other hand, $D \ll -J_K$ leads to $b \gg a$, and the impurity spin is fully polarized in either direction. In both limits, the impurity and the conduction spins are disentangled and the screening is lost, but the two-fold degeneracy of the ground state persists.

We now analyze the effects of a transverse anisotropy parametrized by E in Eq. (2). This term can be rewritten as

$$V_E = \frac{E}{2}\left[(S^+)^2 + (S^-)^2\right]. \tag{7}$$

In an isolated quantum spin, this perturbation would mix the $m = \pm 1$ states. However, this is no longer true in our "underscreened Kondo" problem. Let us first consider the two degenerate ground states in Eq. (4), and apply perturbation theory. The first contribution comes from the second-order correction. It is diagonal and has the same sign for both m_s states. This corresponds merely to a constant shift in the energy levels with no splitting. Another way to see this is by applying V_E to the states directly: $V_E|m_s = 1/2\rangle = -b/2|-\downarrow\rangle$, and $V_E|m_s = -1/2\rangle = -b/2|+\uparrow\rangle$. Therefore, V_E acts on separate subspaces and does not mix them. Hence, we conclude that the transverse anisotropy does not modify the general picture described above. The general form of the two degenerate states will now be

$$\begin{aligned} |1\rangle &= \alpha|0\uparrow\rangle + \beta|+\downarrow\rangle + \gamma|-\downarrow\rangle, \\ |2\rangle &= \alpha|0\downarrow\rangle + \beta|-\uparrow\rangle + \gamma|+\uparrow\rangle. \end{aligned} \tag{8}$$

Clearly, for $E = 0$ we obtain $\alpha = a$, $\beta = b$, $\gamma = 0$ and we recover the original $|m_s\rangle$ states.

2. *Residual interactions*

We should point out that strictly speaking the previous discussion does not correspond to the strong-coupling limit of

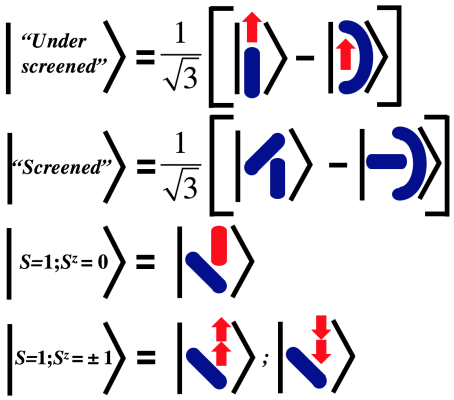

FIG. 3: (color online) Valence bond representation of the single site "Underscreened" spin-doublet state $|m_s = 1/2\rangle$ with one conduction-band electron spin, and of the possible ground states after adding a second conduction spin: "Screened" singlet, and $S_z = 0, \pm 1$ triplet states. The spin-1 impurity is represented as two spins $S = 1/2$. The dangling unscreened spins are shown explicitly and the thick blue(red) lines represent singlets(triplets) between spins-1/2.

the problem. This is studied in Ref. 65 and leads to XXZ anisotropic exchange constants. In addition, one has to account for the rapidly growing anisotropy (in the renormalization group sense) and a residual ferromagnetic coupling between the magnetic impurity and the conduction electrons. We follow Nozières and Blandin's simple arguments[56]: an additional electron would want to increase its kinetic energy by hopping onto the site connected to the impurity. Due to Pauli's exclusion principle, it could only do that if it had the opposite spin orientation, which means the same spin orientation as the impurity spin. Using conventional perturbation theory arguments, this translates into an effective residual ferromagnetic coupling between the impurity spin and the remaining conduction spins.

In order to account for this additional effect, we need to assume a residual interaction between the "Underscreened" states $|m_s = \pm 1/2\rangle$ defined in Eq. (4) and the rest of the Fermi sea. To make these ideas more concrete, we extend the toy model with a second conduction electron spin coupled to the first by an anti-ferromagnetic exchange J, as depicted in Fig. 1(b). We can anticipate that this interaction will counteract J_K, suppressing the magnitude of the magnetic moment of the impurity. More explicitly, we define a new basis: $|0\uparrow\downarrow\rangle, |+\downarrow\downarrow\rangle, |0\downarrow\uparrow\rangle, |-\uparrow\uparrow\rangle$. In this representation, the Hamiltonian is:

$$H = \begin{pmatrix} -\frac{J}{4} & \frac{\sqrt{2}}{2}J_K & \frac{J}{2} & 0 \\ \frac{\sqrt{2}}{2}J_K & -\frac{J_K}{2} + \frac{J}{4} + D & 0 & 0 \\ \frac{J}{2} & 0 & -J/4 & \frac{\sqrt{2}}{2}J_K \\ 0 & 0 & \frac{\sqrt{2}}{2}J_K & -\frac{J_K}{2} + \frac{J}{4} + D \end{pmatrix}. \quad (9)$$

This matrix can be diagonalized to estimate the screening of the impurity moment $\langle S^z_{\rm imp}\rangle$. In Fig. 4(a) we show results for a fixed value $J = 0.2$ and a range of magnetic anisotropies D as a function of J_K. For $J_K \lesssim J$, $D \neq 0$ the quantum

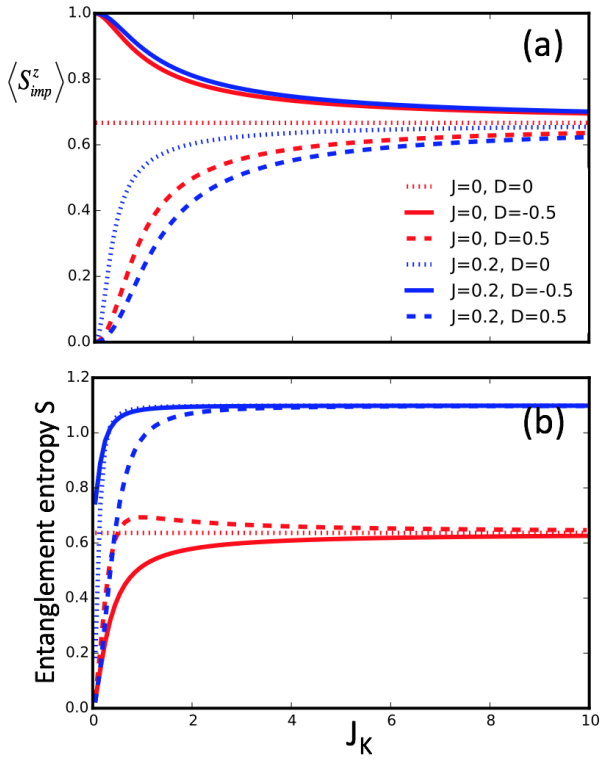

FIG. 4: (a) Impurity magnetic moment $\langle S^z_{\rm imp}\rangle$ for the system of a single $S = 1$ impurity connected to a spin-$1/2$ via J_K, which in turn is connected to a second spin-$1/2$ via J. We consider the ground state in the $S^z = 0$ sector. The antiferromagnetic interaction between the two "conduction" spins competes with the "Kondo" interaction. The effect of J is to induce a residual ferromagnetic coupling between the second conduction spin and the impurity. This coupling tends to reduce the impurity magnetic moment. In the strong coupling limit $\langle S^z_{\rm imp}\rangle \to 2/3$. (b) Entanglement entropy between the impurity spin and the two conduction spins. Even though $\langle S^z_{\rm imp}\rangle$ tends toward the same value in the strong coupling limit, the entanglement entropy clearly distinguishes two different regimes: for finite J the impurity spin is always fully screened, with an asymptotic value $S \to \log 3$. Without J, the impurity is always underscreened, with the entropy converging to $S \to -\frac{1}{3}\log\left(\frac{1}{3}\right) - \frac{2}{3}\log\frac{2}{3}$.

fluctuations are greatly suppressed. For $J_K \gtrsim J$, the values tends toward the value $S^z_{\rm imp} = 2/3$, as expected for the $|m_s = \pm 1/2\rangle$ states.

3. *Magnetic anisotropy effects*

It is instructive to observe the results for the anisotropic case in Fig. 4 more closely. For $D > 0$, $J = 0.2$, they look very similar to the isotropic case. In fact, finite D also tends to force the impurity into the zero magnetization state (for small J_K), enhancing the effects of J and making the residual ferromagnetism more effective. On the other hand, $D < 0$ tends to polarize the spin into the $S^z_{\rm imp} = 1$ orientation. This time the Kondo interaction has to compete against both, the anisotropy,

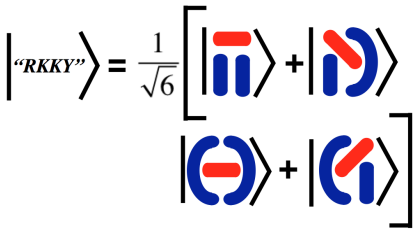

FIG. 5: Illustration of the RKKY state obtained for two impurities and two "conduction spins". Each impurity is coupled to a single conduction electron via J_K, and the conduction electrons are coupled to each other via antiferromagnetic J. The spin-1 impurity is represented as two spins $S = 1/2$. The dangling unscreened spins are shown explicitly and the thick lines represent singlets between spins-1/2. In the ferromagnetic case, the red dimers would be replaced by triplets.

and the J term, to reach the strong interaction value for large J_K.

For small J, one can use first-order degenerate perturbation theory to show that the ground state will be fully screened, *i.e.* $|\text{g.s.}\rangle = 1/\sqrt{2}\,(|m_s = 1/2, \downarrow\rangle - |m_s = -1/2, \uparrow\rangle)$. Here, the extra spin is entangled with the dangling spin into a singlet, shown as the "Screened" state in Fig. 3. We point out that the actual ground state for $D \ll 0$ is in the $S^z = \pm 1$ sectors, with the impurity pointing in either direction, disentangled from the conduction spins, as illustrated by the states $|S = 1; S^z = \pm 1\rangle$ in Fig. 3. These observations will become important in the analysis of the full problem.

We now introduce a transverse anisotropy E through the term (7). If we ignore J, the net effect of V_E is to mix $|m_s = 1/2, \downarrow\rangle$ with $|- \downarrow\rangle$ and $|m_s = -1/2, \uparrow\rangle$ with $|+ \uparrow\rangle$. The coupling J to the third spin will yield a symmetric and antisymmetric linear combination of the two. The states $|- \downarrow\downarrow\rangle, |+ \uparrow\uparrow\rangle$ have unperturbed diagonal energies $J_K/2 + D$. If we assume $E < J_K$ and $D \gg E$, this tunneling barrier is very high and the corrections to the ground state very small. Therefore, once again we conclude that this term does not change the general picture in this parameter regime.

B. Two impurities

In order to provide intuition on the two-impurity problem, we consider two single-impurity "Underscreened" states defined in Eq. (4), and introduce a Heisenberg exchange between the conduction spins. This coupling can be either ferromagnetic or anti-ferromagnetic. Let us fix the total spin projection to $S^z = 0$, in which case we have two degenerate states in the absence of exchange: $|1/2, -1/2\rangle$, and $|-1/2, 1/2\rangle$, where the labels refer to the value of m_s. A simple analysis in terms of degenerate perturbation theory yields an effective Hamiltonian in the form of a 2×2 matrix that can be readily solved to yield that the ground state can be a singlet or a triplet, depending on the sign of the interaction:

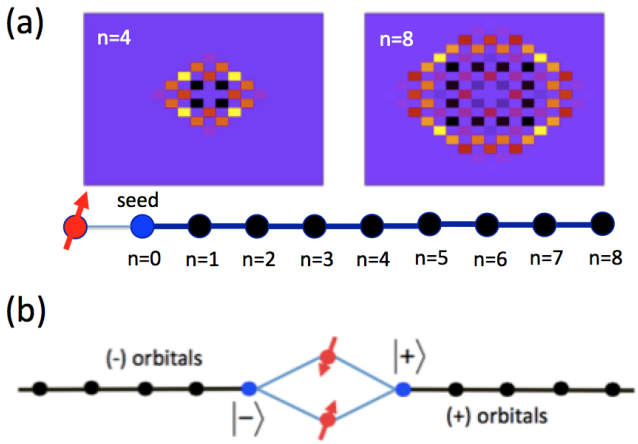

FIG. 6: (a) Chain representation for the single-impurity problem. The bulk non-interacting band structure is mapped via a canonical transformation onto a semi-infinite chain. The impurity is connected to the seed state. We also show the wave function amplitudes for the Lanczos orbitals 4 and 8 in real space. For the two-impurity problem (b), a folding transformation yields one-dimensional bonding and anti-bonding channels. The many-body terms couple the impurities to both.

$$|\text{g.s.}\rangle = \frac{1}{\sqrt{2}}\left(|1/2, -1/2\rangle \pm |-1/2, 1/2\rangle\right). \qquad (10)$$

If we once again represent the spin-1 in terms of two spins-1/2's, one can find that for the isotropic case, this corresponds to an equal superposition of all possible dimer coverings between the dangling spins, as shown in Fig. 5. This indicates that the RKKY state can be interpreted as the unscreened spin becoming maximally entangled. The entanglement entropy between an impurity spin an the rest of the system in this case is $S_{\text{RKKY}} = \log 3$ and the impurity spin is fully screened.

From the ground state expression (10) we find that the spin-spin correlations are simply:

$$\begin{aligned} \langle \text{g.s.}|S_1^x S_2^x + S_1^y S_2^y|\text{g.s.}\rangle &= \pm 4a^2 b^2 \\ \langle \text{g.s.}|S_1^z S_2^z|\text{g.s.}\rangle &= -b^4. \end{aligned} \qquad (11)$$

In the isotropic case these values are $\pm 8/9$ and $4/9$, respectively. In the anisotropic case upon the inclusion of a finite value of D, the $|m_s\rangle$ wave functions will change in character from more Ising-like for $D < 0$, with $b > a$ in (4), to non-magnetic with $a > b$ for $D > 0$. Remarkably, the transverse correlations will reach a maximum value for $D = J_K/2$, since for this case $a = b = 1/\sqrt{2}$, and only then they will start decreasing monotonically with increasing D.

We now comment on the effects of the transverse anisotropy. Assuming that J is the smallest energy scale in the problem, we should solve the single site problem first, and then introduce the RKKY coupling perturbatively. Working in the subspace defined by $|11\rangle, |22\rangle, |21\rangle, |12\rangle$, where the single impurity states $|1\rangle$ and $|2\rangle$ were defined in Eq.(8), we find

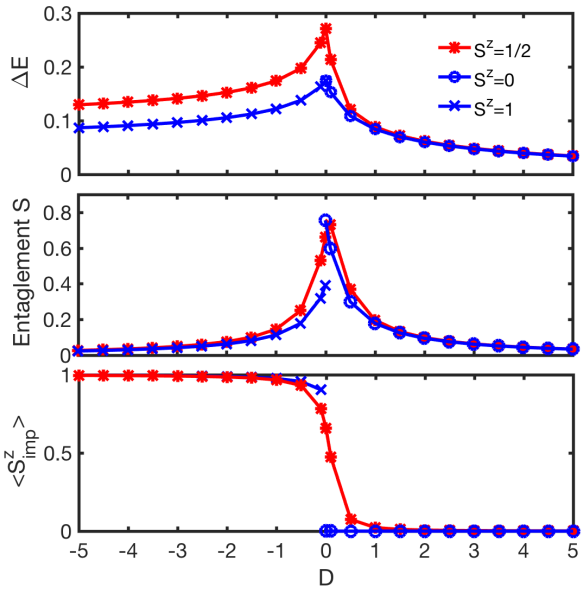

FIG. 7: (a) Energy gain as defined in Eq. (12) for the single-impurity $S = 1$ Kondo problem with J_K = 1 for chain lengths $L = 40$ in the $S^z = 0, 1$ sectors, and $L = 41$ in the $S^z = 1/2$ sector. The $S^z = 1/2$ sector corresponds to an underscreened impurity and is energetically favorable for finite systems. (b) Impurity entanglement entropy and (c) expectation value of the impurity moment, $\langle S^z_{\rm imp}\rangle$, for the same systems and parameters. These results show that for $|D| \gtrsim J_K$ the physical quantities show only very weak even/odd effects, but these are large for $|D| \lesssim J_K$.

that the interaction will only mix $|11\rangle$ with $|22\rangle$ and $|12\rangle$ with $|21\rangle$. If we focus on the last two, the Hamiltonian will be a bi-symmetric 2×2 matrix with eigenstates $1/\sqrt{2}\,(|12\rangle \pm |21\rangle)$, similar to what we had previously, but now with contributions from other spin sectors.

Finally, one should consider the possibility that a strong RKKY interaction may produce a singlet ground state in which the two $S = 1$ impurities lock together directly. In our toy example, this would occur in the case of $J \gg J_K$. In this regime, the conduction electrons lock into a singlet, and one needs to carry out second order perturbation theory in J_K. The result is a particular case of the standard RKKY theory, with an effective coupling between impurities proportional to J_K^2/J. In the extreme limit of the RKKY singlet, the band states are not involved at all, thus there would be entanglement between the two spins, but not between one spin and the band. In this situation, the impurity entanglement entropy would also be $S = \log 3$. However, unlike the RKKY singlet described by Eq. 10, the correlations between impurities would yield a value $\langle S^z_1 S^z_2\rangle$ = -2/3, instead of -4/9.

III. METHODS

A. Single impurity

In order to make the single-impurity problem amenable to DMRG simulations, one needs to apply the unitary transformation described in Ref. 94. The premise is to map the non-interacting lattice Hamiltonian $H_{\rm band}$ in Eq. (1) onto a non-interacting semi-chain, in the same spirit as Wilson's numerical renormalization group method[73,77]. In the absence of a lattice, Wilson chose a basis of partial waves that expand radially away from the impurity. We use a similar approach, in which the basis is built recursively by following a number of very simple steps (we refer the reader to the original proposal[94] for technical details): (i) we define a single-particle seed orbital situated at the site connected to the impurity, (ii) apply the non-interacting Hamiltonian to generate a Krylov basis, and orthogonalize it following a Lanczos procedure. The new single-particle wave functions are orthogonal and connected to each other by a single matrix element. The resulting Hamiltonian in the Lanczos basis will be identical to a semi-infinite chain with site-dependent hoppings, see Fig. 6(a).

We emphasize that this is an exact canonical transformation and that the information about the lattice structure and the hybridization to the impurity is completely preserved. The many-body terms involve only the first site of the chain (the seed orbital) and the impurity, and remain local after the transformation. The resulting one-dimensional problem can be easily solved with the DMRG method, with all numerical errors under control.

Our calculations are conducted on finite systems on the square lattice. One of the remarkable aspects of the mapping is that the size of the chain corresponds to the linear dimension of the original system: a chain of length $L = 50$ represents a square tilted 45 degrees with 100 sites along the diagonal. The "missing" orbitals in the Hilbert space live in different symmetry sectors that do not couple to the impurity (similar to the NRG mapping, where only the s-wave sector is preserved). The fact that the system is finite means that there is an additional important energy scale, the level spacing Δ, which depends on L. For values of the Kondo coupling $J_K < \Delta$ we would find the impurities in the free moment regime, decoupled from the lattice. This is not a problem in the work presented here, since all values of J_K used are large enough.

We point out that the logarithmic van Hove singularity in the square lattice is very mild and does not affect the physics as strongly as a power-law divergence does. For instance, it was found that when the Hubbard model on the square lattice is mapped within the dynamical mean-field theory to an Anderson model with logarithmically diverging density of states at the Fermi level, the Mott metal-insulator transition is not affected[78].

In addition, one has to take another important consideration into account: even and odd effects. In our present case, the correct length that will realize the actual ground state of the problem is not obvious *a priori*, so we resort to studying the energy gained by connecting an impurity with J_K, compared

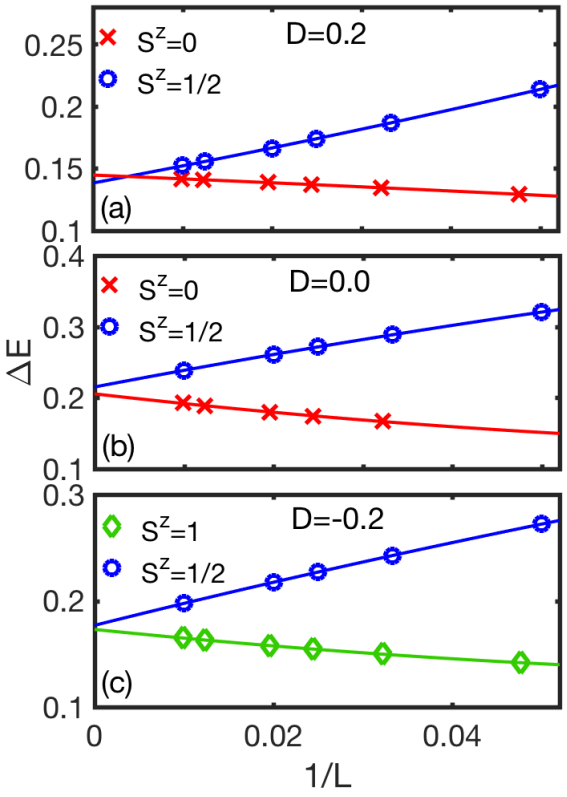

FIG. 8: Scaling of the energy gain ΔE with system size $1/L$ for $J_K = 1$ and (a) $D = 0.2$, (b) $D = 0$ and (c) $D = -0.2$. For finite systems the underscreened state in the $S^z = 1/2$ sector dominates in all three cases. Lines represent quadratic fit in $1/L$. Error bars in the extrapolation are of the order of the symbol size.

to the energy of a disconnected impurity with $J_K = 0$:

$$\Delta E(J_K) = E_0(J_K = 0) - E_0(J_K). \tag{12}$$

The system will typically lower its energy by entangling the impurity to the conduction spins.

The results for fixed $J_K = 1$ as a function of anisotropy D are shown in Fig. 7 and demonstrate that in finite systems odd chains with $S^z = 1/2$ realize a ground state that is energetically favorable. However, for $|D| \gtrsim J_K$ all physical quantities such as the impurity entanglement entropy and $\langle S^z_{\rm imp}\rangle$ are practically indistinguishable regardless of the chain lengths.

As pointed out previously in Section II.A.2., the energy difference is dominated by the residual ferromagnetic interactions that are affected by the inter-level splitting in the non-interacting chains. This can be studied quantitatively by considering the energy gain as a function of systems size for even and odd chain lengths, see Fig. 8. A quadratic fit and $L \to \infty$ extrapolations indicate that the result in the thermodynamic limit is independent of the parity of the chain length, as expected. This is easy to understand: In a chain much longer than the Kondo length, flipping a spin or removing a site from the chain should make no difference in the physical behavior of the impurity. These effects have been elegantly explained in Refs. 79,90, and are a direct consequence of working on

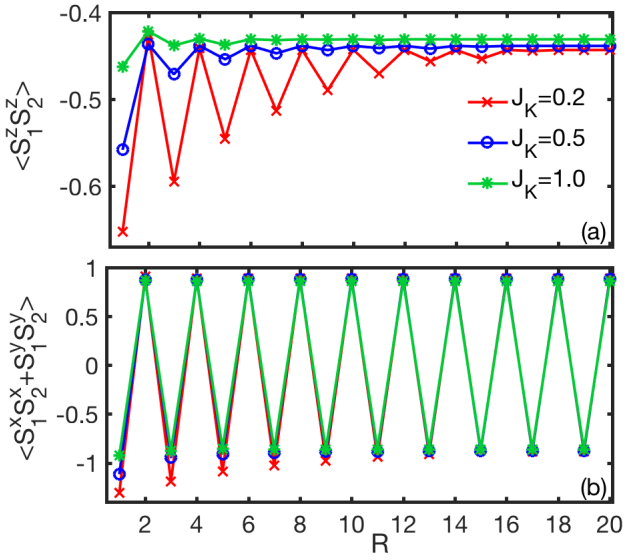

FIG. 9: Diagonal (a) and off-diagonal (b) spin-spin correlations between two spin-1 impurities as a function of their separation R for a range of values of J_K in the $S^z = 0$ sector. We use two chains of length $L = 61$ each.

finite systems. Odd-length chains present a state right at the Fermi level. When we turn on the Kondo interaction and this is smaller or of the order of the level splitting, first-order perturbation theory introduces a direct coupling between the impurity and this electronic state, which is solely responsible for the screening. This is why our description in Section II correctly describes the physics. Even-length chains do not have a state at the Fermi level and the first-order correction vanishes. The energy gain due to the second-order correction is much smaller than that arising from the first-order term. Therefore, the differences seen in Fig. 8 are all a simple consequence of the inter-level spacing in finite chains. These results underscore the importance of carefully handling the even-odd effects on finite systems and indicate that the proper route in finite systems is to take $S^z = 1/2$ for all values of D.

B. Two impurities

In order to generalize the aforementioned procedure to the case of multiple impurities, one applies a Block Lanczos transformation. The resulting Hamiltonian is not block diagonal. In the particular case of two impurities, this corresponds to a ladder-like geometry[80,95–97]. An intuitive picture can be offered as follows: Suppose that we pick two seed orbitals, situated at the positions of the two impurities. We can apply the procedure outlined above for a single impurity: the orbitals will start expanding away from each impurity, generating two one-dimensional chains. At some point, when the length of the chains is $R/2$ (R being the distance between impurities along the lattice axis) the orbitals start overlapping and interfering, translating into terms mixing the two chains, which remain local.

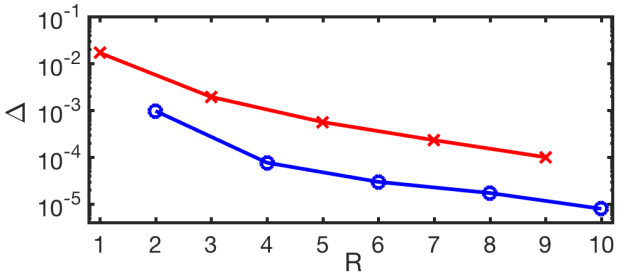

FIG. 10: (color online) Gap from the triplet (singlet) ground state to the first excited state at even distances (blue) and odd distances (red) for $J_K = 1.0, D = E = 0, L = 41$.

We can, however, exploit the reflection symmetry with respect to the centre-point between the two impurities by choosing the seed to be a bonding (symmetric) or anti-bonding (anti-symmetric) linear combination of the original local seeds. For each initial state, the Lanczos iteration procedure is identical to that described in the single-impurity problem[94], with two independent chains, one for each channel, that do not mix. The resulting problem is then truly one-dimensional, see Fig. 6(b). Under this transformation, the many-body interactions are modified: there are terms mixing the impurities and the first orbital of each chain. We note that this symmetrization is identical in spirit and form to the folding transformation used in the NRG calculations for the two-impurity problem,[35] with the main difference being that our symmetrization takes place in real space instead of momentum space. The advantage of this approach is not only that the recursion is greatly simplified, but also that the equivalent one-dimensional problem greatly reduces the entanglement, and thus the computational cost of the simulations.

We consider a square lattice at half filling, mapped so that each chain has an even number of sites. In the DMRG simulations the truncation error was below 10^{-8}, which implies keeping up to 3600 states in some calculations.

IV. RESULTS

A. Isotropic case: $D = 0, E = 0$

In this section we present the results for the spin-1 two-impurity problem in the absence of anisotropy. Based on the intuition established through the studies of the spin-$1/2$ two-impurity problem, two types of behaviors could be expected: formation of two independent Kondo states, or coupling via indirect exchange, with both processes in competition dictated by the relative positions of the two spins and the magnitude of the Kondo interactions J_K. We will show that the spin-1 case is more complex.

In Fig. 9, the spin-spin correlations $\langle S_1^z S_2^z \rangle$ between impurities are shown in the $S^z = 0$ sector as a function of the distance between the impurities, R, for different values of J_K. The spins are positioned along the x axis, therefore even (odd) distances correspond to impurities on the same (opposite) sublattice. Since the RKKY interaction has different character in these two cases, we discuss them separately for clarity.

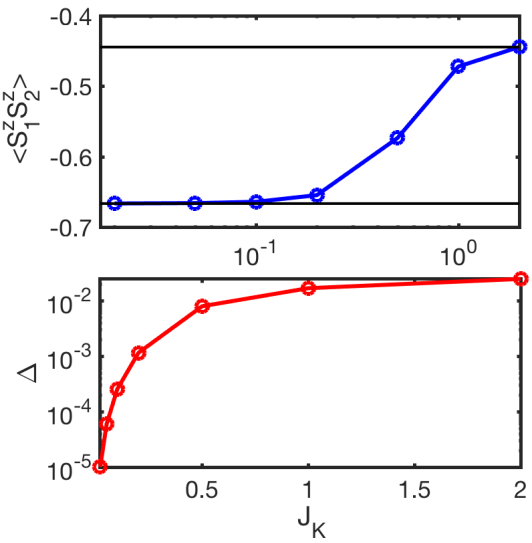

FIG. 11: (a) Spin-spin correlations between impurities at distance $R = 1$ as a function of J_K. The horizontal lines indicate the limiting values -4/9 and -2/3. (b) Singlet-triplet gap between ground-state and first excited state for the same parameters.

1. *Opposite sublattices ($R = 1, 3, \cdots$)*

When impurities are on opposite sublattices, the ground state is a singlet, $S = 0$. As seen in the lower panel of Fig. 9, the magnitude of transverse correlations is twice the value of diagonal correlations, which is a signature of a singlet state. With increasing J_K, the correlations approach algebraically the limiting value of $\langle S_1^z S_2^z \rangle = -(\frac{2}{3})^2 = -4/9$. This result is explained by considering two independent $S = 1$ problems as discussed in Section II A: The case $S^z = 0$, $J_K \to \infty$ can be described as one impurity forming an $m_s = 1/2$ state with a conduction electron, while the other forms an $m_s = -1/2$ state with another conduction electron, resulting in a four-fold degenerate state. From the explicit form of the wave-functions, calculated in Section II A, it follows that the correlations should equal the stated value. The same value is also reached in the large-R limit for any finite value of J_K.

These results show that the dangling spins (residual spin-$1/2$ local moments) couple anti-ferromagnetically through the indirect RKKY exchange. This means that, unlike in the case of spin-1/2 Kondo impurities, *Kondo and RKKY physics coexist*.

Remarkably, at short distance $R = 1$ and for small interaction J_K we find that the correlations tend to the RKKY limit $\langle S_1^z S_2^z \rangle = -2/3$. In order to understand this behavior we studied the J_K dependence of the correlations, as shown in Fig. 11. Even though the entanglement entropy remains constant $S = \log 3$, the results indicate a crossover from an RKKY singlet with two $S = 1$ impurities locked together for small J_K, to a "Kondo+RKKY" state at large J_K, with

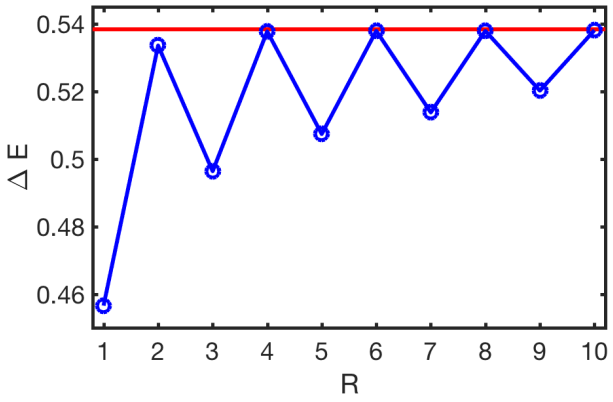

FIG. 12: Energy gain for two $S = 1$ impurities as a function of distance, for $J_K = 1, L = 41$. The horizontal line represents the value for two independent impurities at infinite distance.

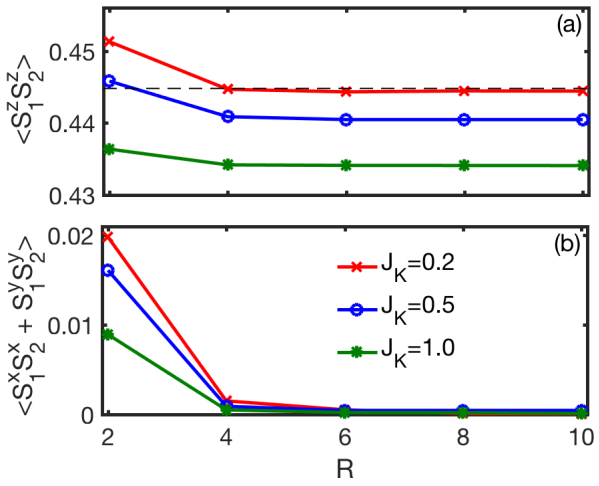

FIG. 13: Spin-spin correlations between two spin-1 impurities as a function of their separation for a range of values of J_K in the $S^z = 1$ sector. The horizontal dashed line indicates the value of $4/9$. We only show even sites, corresponding to a triplet ground state. $L = 61$.

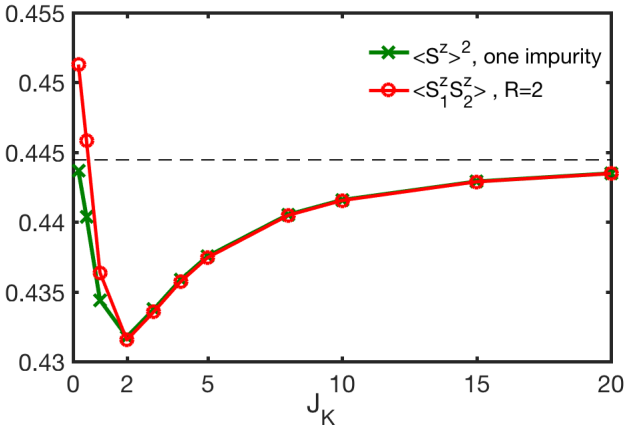

FIG. 14: Spin-correlation between two impurities at fixed separation $R = 2$ as a function of the Kondo coupling J_K. The single-impurity moment squared, $\langle S^z \rangle^2$, is also shown for comparison. For $J_K > 2$, the two lines are almost indistinguishable, indicating two essentially uncorrelated underscreened impurities. The chain lengths are $L = 84$ and $L = 40$ for the two-impurity and single-impurity cases, respectively.

the correlations evolving from $-2/3$ to $-4/9$ as the singlet-triplet gap increases. This is in agreement with our analysis in Section II B.

2. *Same sublattice ($R = 2, 4, \cdots$)*

Impurities on the same sublattice yield a triplet ground state. However, the gap to the excited non-degenerate singlet state is quite small. Calculations were done with high energy precision and varying system sizes, $L = 21, 41$ and 61 (where L is the size of each non-interacting chain without the impurity), confirming that this gap is not a numerical artifact. The splitting decreases with increasing impurity separation, as seen in Fig. 10, and barely changes with chain size. The system is gapless in the thermodynamic limit: flipping the spin of an electron very far from the impurity should not affect the physics. But this finite-size gap is dictated by the level splitting in the bulk, which is much larger than the singlet-triplet gap measured in this plot. We interpret this result as follows: the two impurities form a triplet (or singlet, depending on the sublattice) state mediated by the RKKY interaction. In a similar fashion as Nozières's Fermi liquid picture for the single impurity Kondo problem, this "bound state" acts as a scattering center for the conduction electrons that form an orthogonal Fermi sea (notice that in the chain representation, the two impurities are localized). The internal structure of the RKKY state is as depicted by Fig. 5 and Eq. 10. From our discussion in Section II B we learn that the singlet-triplet gap is dictated by the residual interactions with the conduction electrons that are responsible for mediating the RKKY exchange.

Fig. 12 shows the energy gain for two impurities obtained using Eq.(12) with $J_K = 1$. This quantity provides information about the correlation energy. We notice that for impurities on the same sublattice and for sufficiently large R, ΔE approaches a constant value: twice the energy gain for a single impurity. This indicates that they tend to form two independent Kondo clouds, oblivious to the presence of the other spin and with the consequent four-fold degeneracy due to the two dangling spin 1/2's pointing in arbitrary directions. This occurs already at relatively short distances and is a remarkable aspect of the two impurity problem on a half-filled bipartite lattice: the electronic wave functions have nodes at the position of the second impurity hindering the possibility of mediating an indirect RKKY exchange[80]. The energy gain, or correlation energy (Fig. 12) combines the contributions from the partial Kondo screening (proportional to $T_K \sim J_K \exp(-1/\rho J_K) \approx J_K$) and the RKKY interaction. Therefore, it is not the energy gain, but the finite-size gap (Fig. 10) that yields a measure of J_{RKKY}.

Rigorously, the strict ground state at even distances is per-

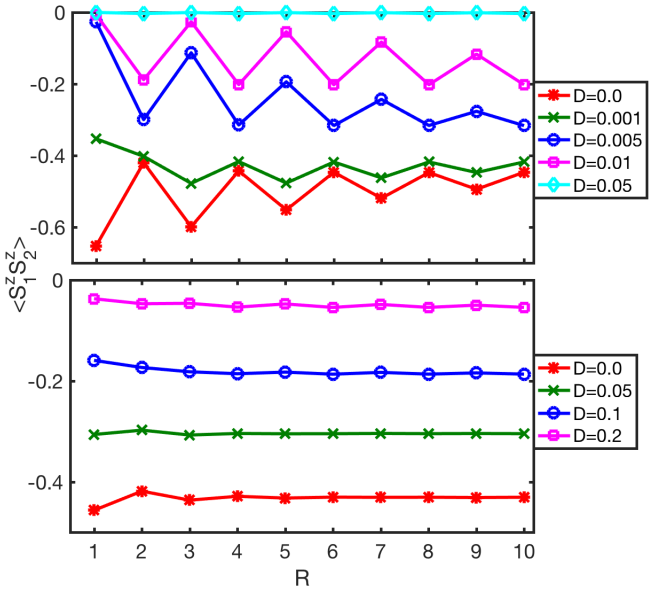

FIG. 15: Spin-correlations between two spin-1 impurities as a function of their separation R for different values of longitudinal magnetic anisotropy $D > 0$ with $J_K = 0.2$ (top) and $J_K = 1.0$ (bottom). Here $L = 104$.

fectly described in terms of two entangled Kondo states forming a triplet, as obtained in Section II B. Due to the choice of $S^z = 0$ in the DMRG calculations, we cannot observe ferromagnetic alignment in the diagonal correlations, however the off-diagonal correlations are *minus* twice the value of the diagonal ones, which is a signature of a triplet state (see Fig. 9). Since the system is degenerate, we can also consider the ground-state in the $S^z = 1$ sector (Fig. 13) to confirm this interpretation. In this case, the dangling spins point in the same direction and we expect the correlations in the z-direction to converge to $b^4 = (\frac{2}{3})^2$, which is indeed observed in Fig. 13.

Interestingly, the correlations only saturate to $(\frac{2}{3})^2$ in the strong-coupling limit and have a non-monotonic behavior as a function of J_K. This is highlighted in Fig. 14 for distance $R = 2$. The reason the correlations dip below $(\frac{2}{3})^2$ is the residual ferromagnetic coupling of the spin-1 Kondo effect. This is a well-known single-impurity phenomenon. At weak coupling, the residual ferromagnetic interaction with the conduction electrons reduces the absolute value of the correlations[56]. Upon increasing J_K, the system tends toward the strong coupling limit and the residual ferromagnetism disappears. However, the impurities completely disentangle before that limit is reached: at values of $J_K > 2$ the spin-spin correlations are $\langle S_1^z S_2^z \rangle = \langle S_{\rm imp}^z \rangle^2$, where $\langle S_{\rm imp}^z \rangle$ is the result for a single impurity. The same effect would be seen for odd distances, with the difference being that the correlations are negative.

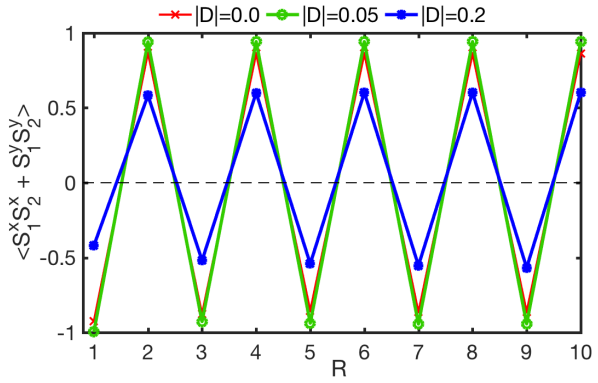

FIG. 16: Spin-correlations in the transverse direction for $J_K = 1.0$ with $D > 0$.

B. Anisotropic case: $D \neq 0$, $E = 0$

Once magnetic anisotropy is included (Eq. 2), the impurities display different behavior depending on the sign of D. For clarity we discuss the two cases separately.

1. $D > 0$

When the anisotropy is positive, the ground state has $S^z = 0$ regardless of what sublattice the impurities are coupled to. Fig .15 shows the z-component of the correlations for a small ($J_K = 0.2$) and large ($J_K = 1.0$) coupling. For positive D, the impurity spin gets suppressed and the correlations shift monotonically to zero. We do not observe ferromagnetism in the longitudinal direction and the correlations remain always antiferromagnetic, irrespective of distance.

In all cases, the correlations at long distances plateau at a constant value $\langle S_1^z S_2^z \rangle \to -b^4$ that depends on J_K and D. Moreover, for impurities on the same sublattice we find that the ground state and the first excited state are quasi degenerate, with a gap of the order of 10^{-5} or smaller, indicating that the two dangling spins are practically uncorrelated. As discussed in the isotropic case, the dangling spins may point in either direction, leading to a four-fold (quasi) degeneracy.

Due to the anisotropy, the correlations have different behavior in the transverse direction, as seen in Fig. 16. We first notice that for small values of $D > 0$ the magnitude of the correlations *increases*. This was already observed in Sec.II B for the simple case of two sites. For large $|D|$, the correlations decay to zero, indicating the suppression of the quantum fluctuations. In addition, we can see the character of the RKKY interaction, oscillating between ferromagnetic and antiferromagnetic depending on the sublattice.

2. $D < 0$

We switch now to the case of $D < 0$. In this situation, the ground state has $S^z = 0$ if impurities are on opposite sublattices, and $S^z = \pm 1$ when on the same sublattice. Results

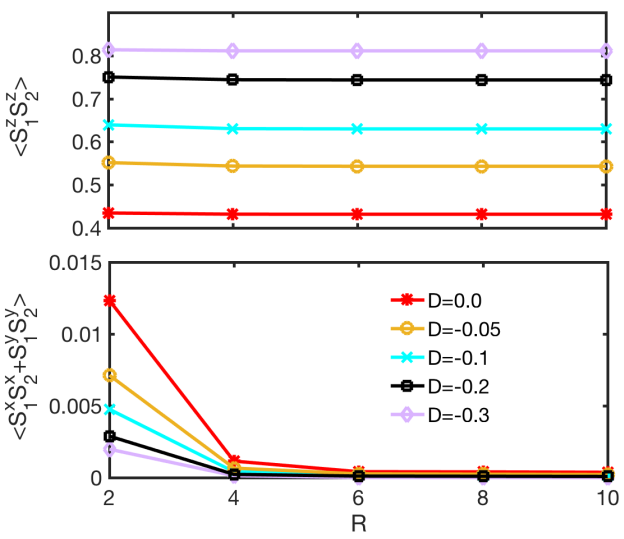

FIG. 17: Longitudinal (top) and transverse (bottom) spin-correlations for $J_K = 1.0$ with $D < 0$ at even distances for $S^z = 1$.

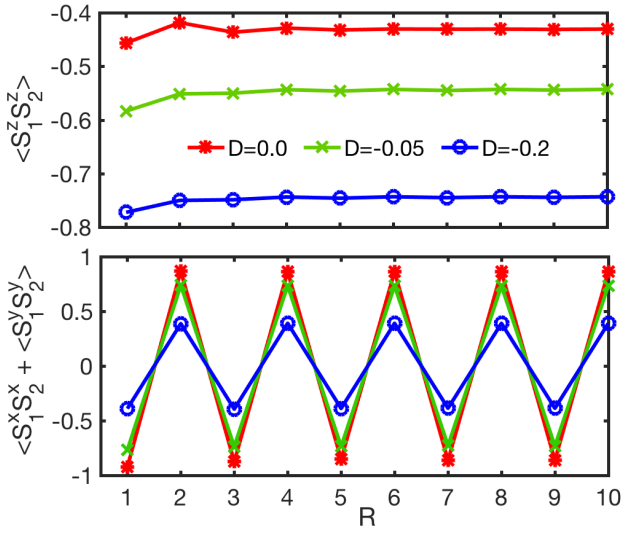

FIG. 18: Longitudinal (top) and transverse (bottom) spin-correlations for $J_K = 1.0$ with $D < 0$ with $S^z = 0$.

for even distances are shown in Fig. 17. Here, the impurities tend to align with increasing D, approaching the values $\langle S_1^z S_2^z \rangle = 1$ and $\langle S_1^x S_2^x \rangle = 0$, as expected from Ising spins. The same argument applies to odd distances. In this case, the impurities are anti-aligned but still behaving as Ising spins as $D \to -\infty$, as seen in Fig. 18. Results for even distances in the $S^z = 0$ sector are shown for comparison. Again these states could be described as *quasi*-degenerate, with the gap on the order of 10^{-5}.

3. *Characterization through entanglement*

The screening process can be characterized through the entanglement between one impurity spin and the rest of the system, shown in Fig. 19, together with the spin correlations. We considered the impurities at distance $R = 2$ and $J_K = 1$, with chains of size $L = 51$. Magnetic anisotropy (finite D) tends to kill the spin fluctuations. For sufficiently large $D < 0$ the impurities behave as Ising spins. For $D > 0$ the impurities become practically uncorrelated in the z-direction, but antiferromagnetic correlations survive in the transverse direction. This is consistent with the renormalization group analysis[65] that indicates that the system should develop a dominant transverse anisotropy for $D > 0$.

C. Transverse anisotropy: $D < 0$, $E \neq 0$

Including the transverse anisotropy term E, see Eq. (7), mixes subspaces with different total S^z, making calculations considerably costlier. We looked at one particular case, for parameters $J_K = 1.0, D = -0.2, E = 0.05$ and calculated the spin-spin correlations as a function of the inter-impurity distance, shown in Fig. 20. In this case, the ground state is always non-degenerate but the gap still remains very small when the spins are on the same sublattice and decreases with the inter-impurity distance. This indicates that for even distances we still have an $S = 1/2$ degree of freedom that practically remains dangling. The effects of the transverse anisotropy are quite dramatic, when comparing to Figs. 15 and 16: The transverse correlations, even though they preserve the same structure, are considerably reduced, while the longitudinal one now present the character proper of the RKKY interaction and oscillate between ferro and anti-ferromagnetic. This oscillation is now observable because the interaction is mixing states with impurities pointing in either direction.

V. CONCLUSIONS

We have conducted an extensive study of the two-impurity Kondo problem for spin-1 adatoms on square lattice. We provided a simple intuitive picture and identified the different regimes, depending on system size, Kondo coupling J_K and magnetic anisotropy. For two impurities, the nature and properties of the ground state depend most importantly on the spins being on the same or opposite sublattices. Impurities on opposite (same) sublattice have a singlet (triplet) ground state. However, the energy difference between the triplet ground state and the singlet excited state is very small and we expect a four-fold degenerate ground state for impurities on the same sublattice. For large enough J_K the impurities become completely uncorrelated forming two independent underscreened states with the conduction electrons.

Interestingly, our calculations support a picture in which underscreening (Kondo) and RKKY correlations coexist: conduction electron partially screen the individual impurities, and the dangling $S = 1/2$ degree of freedoms are responsible for establishing RKKY correlations between them. One should be mindful that the effective energy scale in the problem J_{RKKY} is typically smaller than the finite-size level splitting.

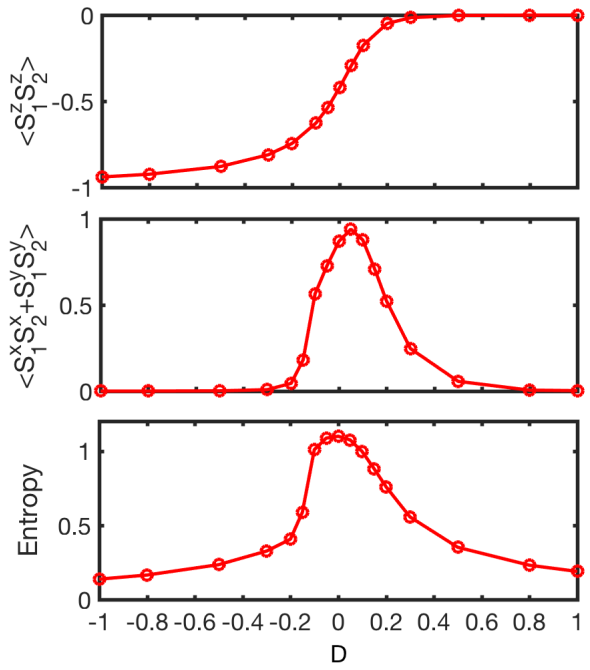

FIG. 19: (a) Diagonal and (b) off-diagonal spin-spin correlations between impurities at distance $R = 2$ for $J_K = 1$ as a function of magnetic anisotropy D and for $S^z = 0$. We show results for chains of length $L = 2n + 1$. (c) Entanglement entropy for one of the impurities, obtained by tracing over the rest of the system.

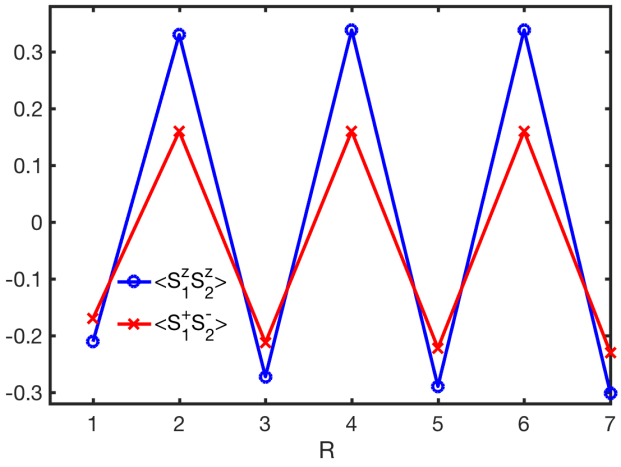

FIG. 20: Diagonal and transverse spin-spin correlations for impurities at different distances and parameters $J_K = 1.0, D = -0.2, E = 0.05$.

There is a possibility that a more complex behavior might emerge as a result when both quantities become comparable.

In order for the impurities to realize quasi-classical behavior we need to go to the large $D < 0$ limit. For anisotropies of the order of the Kondo coupling the impurities always display an important amount of entanglement. The dependence of the entanglement and correlations with system size indicate that this behavior could be realized in experiments by electrostatically confining the impurity to an "electron puddle" (Kondo box) and varying the size of the confining potential around the impurity.

Acknowledgments

We thank C. Hirjibejedin for useful and stimulating conversations. AEF and AA are greateful to the U.S. Department of Energy, Office of Basic Energy Sciences, for support under grant DE-SC0014407. RŽ acknowledges the support of the Slovenian Research Agency (ARRS) under P1-0044 and J1-7259.

[1] F. Donati, L. Gragnaniello, a. Cavallin, F. Natterer, Q. Dubout, M. Pivetta, F. Patthey, J. Dreiser, C. Piamonteze, S. Rusponi, et al., Phys. Rev. Lett. **113**, 177201.
[2] J. Hu, J. Alicea, R. Wu, and M. Franz, Phys. Rev. Lett. **109**, 266801 (2012).
[3] R. Drost, T. Ojanen, A. Harju, and P. Liljeroth, Nat. Phys. **13**, 668 (2017).
[4] a. Enders, R. Skomski, and J. Honolka, J. Phys. Condens. Matter **22**, 433001 (2010).
[5] M. N. Leuenberger and D. Loss, Nature **410**, 789 (2001).
[6] A. Ardavan, O. Rival, J. J. L. Morton, S. J. Blundell, A. M. Tyryshkin, G. A. Timco, and R. E. P. Winpenny, Phys. Rev. Lett.

98, 057201 (2007).
[7] C. Karlewski, M. Marthaler, T. Märkl, T. Balashov, W. Wulfhekel, and G. Schön, Phys. Rev. B **91**, 245430 (2015).
[8] D. Serrate, P. Ferriani, Y. Yoshida, S.-w. Hla, M. Menzel, K. V. Bergmann, S. Heinze, A. Kubetzka, and R. Wiesendanger, Nat. Nanotechnol. **5**, 350 (2010).
[9] F. Donati, S. Rusponi, S. Stepanow, A. Singha, L. Persichetti, R. Baltic, K. Diller, F. Patthey, E. Fernandes, J. Dreiser, et al., Science (80-.). **352**, 318 (2016).
[10] F. D. Natterer, K. Yang, W. Paul, P. Willke, T. Choi, T. Greber, and A. J. Heinrich, Nature **543**, 226 (2017).
[11] M. F. Crommie, C. P. Lutz, and D. M. Eigler, Science **262**, 218 (1993).
[12] Y. Hasegawa and P. Avouris, Phys. Rev. Lett. **71**, 1071 (1993).
[13] S. Loth, S. Baumann, C. P. Lutz, D. M. Eigler, and A. J. Heinrich, Science **335**, 196 (2012).
[14] J. Lagoute, C. Nacci, and S. Fölsch, Phys. Rev. Lett. **98**, 146804 (2007).
[15] N. Néel, R. Berndt, J. Kröger, T. O. Wehling, A. I. Lichtenstein, and M. I. Katsnelson, Phys. Rev. Lett. **107**, 106804 (2011).
[16] W. Chen, T. Jamneala, V. Madhavan, and M. F. Crommie, Phys. Rev. B **60**, 8529 (1999).
[17] A. F. Otte, M. Ternes, K. von Bergmann, S. Loth, H. Brune, C. P. Lutz, C. F. Hirjibehedin, and A. J. Heinrich, Nat. Phys. **4**, 847 (2008).
[18] L. Zhou, J. Wiebe, S. Lounis, E. Vedmedenko, F. Meier, S. Blügel, P. H. Dederichs, and R. Wiesendanger, Nat. Phys. **6**, 187 (2010).
[19] H. Prüser, M. Wenderoth, P. E. Dargel, A. Weismann, R. Peters, T. Pruschke, and R. G. Ulbrich, Nat. Phys. **7**, 7 (2011).
[20] H. Prüser, P. E. Dargel, M. Bouhassoune, R. G. Ulbrich, T. Pruschke, S. Lounis, and M. Wenderoth, Nat. Commun. **5**, 5417 (2014).
[21] H. C. Manoharan, C. P. Lutz, and D. M. Eigler, Nature **403**, 512 (2000).
[22] A. A. Khajetoorians, J. Wiebe, B. Chilian, S. Lounis, S. Blügel, and R. Wiesendanger, Nat. Phys. **8**, 497 (2012).
[23] R. Wiesendanger, Rev. Mod. Phys. **81**, 1495 (2009).
[24] A. A. Khajetoorians, J. Wiebe, C. Bruno, S. Lounis, S. Blügel, and R. Wiesendanger, Nature Physics **8** (2012).
[25] A. Spinelli, M. P. Rebergen, and A. F. Otte, J. Phys Condens. Matter **27**, 243203 (2015).
[26] D. Bercioux and S. Otte, Nat. Phys. **13**, 628 (2017).
[27] C. F. Hirjibehedin, C.-Y. Lin, A. F. Otte, M. Ternes, C. P. Lutz, B. A. Jones, and A. J. Heinrich, Science **317**, 1199 (2007).
[28] J. C. Oberg, M. R. Calvo, F. Delgado, M. Moro-Lagares, D. Serrate, D. Jacob, J. Fernandez-Rossier, and C. F. Hirjibehedin, Nat Nano **9**, 64 (2013).
[29] A. Hewson, *The Kondo Problem to Heavy Fermions* (Cambridge Univ. Press, 1997).
[30] M. A. Rudermann and C. Kittel, Phys. Rev. **96**, 99 (1954).
[31] T. Kasuya, T. Prog. Theor. Phys. **16**, 45 (1956).
[32] K. Yosida, Phys. Rev. **106**, 893 (1957).
[33] S. Doniach, Physica B **91**, 231 (1977).
[34] B. A. Jones, C. M. Varma, and J. W. Wilkins, Phys. Rev. Lett. **61**, 125 (1988).
[35] B. A. Jones, B. G. Kotliar, and A. J. Millis, Phys. Rev. B **39**, 3415 (1989).
[36] G. Zaránd, C.-H. Chung, P. Simon, and M. Vojta, Phys. Rev. Lett. **97**, 166802 (2006).
[37] K. Ingersent, A. W. W. Ludwig, and I. Affleck, Phys. Rev. Lett. **95**, 257204 (2005).
[38] C. Jayaprakash, H. R. Krishna-murthy, and J. W. Wilkins, Phys. Rev. Lett. **47**, 737 (1981).
[39] R. M. Fye, J. E. Hirsch, and D. J. Scalapino, Phys. Rev. B **35**, 4901 (1987).
[40] B. A. Jones and C. M. Varma, Phys. Rev. Lett. **58**, 843 (1987).
[41] B. A. Jones and C. M. Varma, Phys. Rev. B **40**, 324 (1989).
[42] I. Affleck and A. W. W. Ludwig, Phys. Rev. Lett. **68**, 1046 (1992).
[43] C. Sire, C. M. Varma, and H. R. Krishnamurthy, Phys. Rev. B **48**, 13833 (1993).
[44] I. Affleck, A. W. W. Ludwig, and B. A. Jones, Phys. Rev. B **52**, 9528 (1995).
[45] J. Gan, Phys. Rev. Lett. **74**, 2583 (1995).
[46] J. B. Silva, W. L. C. Lima, W. C. Oliveira, J. L. N. Mello, L. N. Oliveira, and J. W. Wilkins, Phys. Rev. Lett. **76**, 275 (1996).
[47] A. Georges and Y. Meir, Phys. Rev. Lett. **82**, 3508 (1999).
[48] W. Izumida and O. Sakai, Phys. Rev. B **62**, 10260 (2000).
[49] R. López, R. Aguado, and G. Platero, Phys. Rev. Lett. **89**, 136802 (2002).
[50] R. Aguado and D. C. Langreth, Phys. Rev. B **67**, 245307 (2003).
[51] P. Simon, R. López, and Y. Oreg, Phys. Rev. Lett. **94**, 086602 (2005).
[52] H. Jeong, A. M. Chang, and M. R. Melloch, Science **293**, 2221 (2001).
[53] N. J. Craig, J. M. Taylor, E. A. Lester, C. M. Marcus, M. P. Hanson, and A. C. Gossard, Science **304**, 565 (2004).
[54] P. Wahl, P. Simon, L. Diekhöner, V. S. Stepanyuk, P. Bruno, M. A. Schneider, and K. Kern, Phys. Rev. Lett. **98**, 056601 (2007).
[55] D. C. Mattis, Phys. Rev. Lett. **19**, 1478 (1967).
[56] P. Nozieres and A. Blandin, J. Phys. **41**, 193 (1980).
[57] V. A. Fateev and P. B. Wiegmann, Phys. Rev. Lett. **46**, 1595 (1981).
[58] V. A. Fateev and P. B. Wiegmann, Phys. Lett. **81**, 179 (1981).
[59] K. Furuya and J. H. Lowenstein, Phys. Rev. B **25**, 5935 (1982).
[60] N. Andrei, K. Furuya, and J. Lowenstein, Rev. Mod. Phys. **55**, 331 (1983).
[61] D. M. Cragg and P. Lloyd, J. Phys. C Solid State Phys. **12**, L215 (1979).
[62] P. Lloyd, A. W. Mirtschin, D. M. Cragg, D. M. Cragg, P. Lloyd, D. M. Cragg, P. Lloyd, A. W. Mirtschin, P. Lloyd, P. Lloyd, et al., J. Phys. C Solid State Phys. **13**, 803 (1980).
[63] P. Mehta, N. Andrei, P. Coleman, L. Borda, and G. Zarand, Phys. Rev. B **72**, 014430 (2005).
[64] W. Koller, A. C. Hewson, and D. Meyer, Phys. Rev. B **72**, 045117 (2005).
[65] R. Žitko, R. Peters, and T. Pruschke, Phys. Rev. B **78**, 224404, (2008).
[66] P. Coleman and C. Pépin, Phys. Rev. B **68**, 220405(R) (2003).
[67] D. E. Logan, A. P. Tucker, and M. R. Galpin, Phys. Rev. B **90**, 075150 (2014).
[68] O. Ujsaghy and A. Zawadowski, Phys. Rev. B **60**, 10602 (1999).
[69] L. Szunyogh, G. Zarand, S. Gallego, M. C. Muñoz, and B. L. Györffy, Phys. Rev. Lett. **96**, 067204 (2006).
[70] C. Etz, J. Zabloudil, and P. Weinberger, E. Y.. Vedmedenko, Phys. Rev. B **77** 184425 (2008).
[71] F. Delgado and J. Fernández-Rossier, Prog. Surf. Sci. **92**, 40 (2017).
[72] A. F. Otte, M. Ternes, K. von Bergmann, S. Loth, H. Brune, C. P. Lutz, C. F. Hirjibehedin, and A. J. Heinrich, Nat Phys **4**, 847 (2008).
[73] K. G. Wilson, Rev. Mod. Phys. **47**, 773 (1975).
[74] N. Andrei, Phys. Rev. Lett. **45**, 379 (1980).
[75] A. Tsvelik and P. Wiegmann, J. Phys. C:Solid State Phys. **16**, 2281 (1983).
[76] A. Tsvelik and P. Wiegmann, J. Phys. C:Solid State Phys. **16**, 2321 (1983).
[77] R. Bulla, T. A. Costi, and T. Pruschke, Rev. Mod. Phys. **80**, 395 (2008).

[78] Rok Žitko, Janez Bonča, and Thomas Pruschke, Phys. Rev. B **80**, 245112 (2009).
[79] A. Schwabe, D. Gütersloh, and M. Potthoff, Phys. Rev. Lett. **109**, 257202 (2012).
[80] A. Allerdt, C. A. Büsser, G. B. Martins, and A. E. Feiguin, Phys. Rev. B **91**, 085101 (2015).
[81] A. K. Mitchell, P. G. Derry, and D. E. Logan, Phys. Rev. B **91**, 235127 (2015).
[82] A. Schwabe, M. Hänsel, M. Potthoff, and A. K. Mitchell, Phys. Rev. B **92**, 155104 (2015).
[83] S. R. White, Phys. Rev. Lett. **69**, 2863 (1992).
[84] S. R. White, Phys. Rev. B **48**, 10345 (1993).
[85] U. Schollwöck, Rev. Mod. Phys. **77**, 259 (2005).
[86] O. Sakai, Y. Shimizu, and T. Kasuya, Solid State Communications **75**, 81 (1990).
[87] O. Sakai, and Y. Shimizu, Journal of the Physical Society of Japan **61**, 2333 (1992).
[88] J. B. Silva, W. L. C. Lima, W. C. Oliveira, J. L. N. Mello, L. N. Oliveira, and J. W. Wilkins, Phys. Rev. Lett. **76**, 275 (1996).
[89] L. Zhu, and J. X. Zhu, Phys. Rev. B **83**, 195103 (2011).
[90] C. Yang and A. E. Feiguin, Phys. Rev. B **95**, 115106 (2017).
[91] Andrew K. Mitchell, Thomas F. Jarrold, and David E. Logan, Phys. Rev. B **79**, 085124 (2009).
[92] E. Vernek, P. A. Orellana, and S. E. Ulloa, Phys. Rev. B **82**, 165304 (2010).
[93] P. P. Baruselli, R. Requist, M. Fabrizio, and E. Tosatti, Phys. Rev. Lett. **111**, 047201 (2013).
[94] C. A. Büsser, G. B. Martins, and A. E. Feiguin, Phys. Rev. B **88**, 245113 (2013).
[95] A. Allerdt, A. E. Feiguin, and S. Das Sarma, Phys. Rev. B **95**, 104402 (2017).
[96] A. Allerdt, R. Žitko, and A. E. Feiguin, Phys. Rev. B **95**, 235416 (2017).
[97] A. Allerdt, A. E. Feiguin, and G. B. Martins, Phys. Rev. B **96**, 035109 (2017).